Bull. Chem. Soc. Ethiop. **2024**, 38(5), 1493-1507.
DOI: https://dx.doi.org/10.4314/bcse.v38i5.23

ISSN 1011-3924
Printed in Ethiopia
Online ISSN 1726-801X

INVESTIGATION ON SULFUR SUBSTITUTED CADMIUM IONS WITH SUPERHYDROPHOBIC NATURE AND LONG-TERM ANTICORROSION PERFORMANCE

Sultan Althahban[1], Mohammed Kuku[1], Yosef Jazaa[2,3] and Haewon Byeon[4*]

[1]Department of Mechanical Engineering, Jazan University, Jazan 82822, Saudi Arabia
[2]Department of Mechanical Engineering, College of Engineering, King Khalid University, P.O. Box 394, Abha 61421, Saudi Arabia
[3]Center for Engineering and Technology Innovations, King Khalid University, Abha 61421, Saudi Arabia
[4]Inje University, Medical Big Data Research Center, Gimhae 50834, South Korea

(Received April 22, 2024; Revised May 12, 2024; Accepted May 23, 2024)

ABSTRACT. Cadmium sulfide nanoparticles (CdS) were effectively prepared using ultrasonication-assisted synthesis. The high hydrophobicity and excellent dispersibility of the synthesised CdS nanoparticles in ethanol could increase their anti-penetrant effect against corrosive media. We evaluated and examined the corrosion prevention properties of CdS nanoparticle coatings on MS steel using Tafel polarisation and electrochemical impedance spectroscopy in HCl, NaCl, and KOH. The experimental results demonstrated that CdS nanoparticle coatings had higher corrosion performance than uncoated MS plates. Besides, CdS nanoparticles may be adsorbed on steel to produce a hydrophobic anti-corrosion layer, enhancing corrosion resistance. The impedance of CdS coatings increased continuously during electrolyte immersion. The results show that CdS acted as a suitable inhibitor and this inhibition efficiency and the polarization curves indicated that CdS nanoparticles performed as mixed inhibitors. The inhibition effect on the surface of the MS plate using CdS nanoparticle coating was investigated with inhibitors confirmed by nanoindentation techniques. The revolutionary approach for creating hydrophobic CdS nanoparticles suggested in this exertion may stimulate the development of high-performance anticorrosion materials and their corrosive protection applications.

KEY WORDS: CdS nanoparticles, Mild steel plate coating, Anticorrosion applications

INTRODUCTION

Corrosion is a widespread and persistent problem that affects various materials, particularly metals and alloys, when exposed to environmental conditions. It is a complex electrochemical process that can lead to the gradual deterioration and degradation of materials over time resulting from chemical interactions with the surrounding environment, continues to pose a significant and widespread problem in several sectors, including industries, infrastructures, and daily activities [1]. Researchers are motivated to constantly explore novel approaches for preventing and reducing the rate of corrosion due to its serious consequences, which include economic losses, weakened safety, and adverse environmental effects.

The objective of synthesizing novel materials for efficient anticorrosion is a promising route, particularly cadmium sulfide (CdS) emerging as a unique material of increasing significance. The CdS is a compound composed of the elements cadmium (Cd) and sulfur (S); it exhibits unique properties that make it a compelling candidate for anticorrosion coatings [2]. The nanocrystalline CdS is an II–VI semiconductor with size-dependent properties, excellent chemical stability, electrical conductivity, and resistance to harsh environmental conditions make it attractive for protecting metals and alloys from corrosion [3]. Additionally, the remarkable semiconducting properties and photoactivity of CdS have led to its use in various technological applications,

*Corresponding authors. E-mail: haewonbyeonr@gmail.com; bhwpuma@naver.com

including solar cells and photocatalysis. It also exhibits excellent chemical stability and resistant to oxidation, a significant advantage when used as an anticorrosion coating or additive due to its unique properties. The CdS can also be applied as a protective coating on metal structures surface and components susceptible to corrosion [4]. This coating acts as a barrier, preventing the metal substrate from directly contacting corrosive environmental elements, such as moisture and chemicals. Also, it creates a barrier that inhibits the diffusion of water and oxygen, both of which are essential for many corrosion processes. By blocking the ingress of these elements, CdS helps to slow down or prevent the corrosion of metal surfaces [5]. Moreover, its chemical stability and resistance to environmental factors make it a valuable tool in mitigating corrosion and extending the lifespan of metal structures and components. One such technique that has been used is the synthesis of cadmium sulfide (CdS) by applying the sonochemical process. Sonication is a process that exploits high-frequency sound waves (ultrasound) to produce mechanical vibrations in a liquid medium [6]. It is used for homogenizing and dispersing particles in liquids. It can break down agglomerates and improve the uniformity of suspensions, emulsions, and dispersions. The utilization of this method has several benefits, including rapid reaction kinetics, precise regulation of particle dimensions and structure, and the capacity to produce materials at comparably lower temperatures. The characteristics mentioned above make sonochemistry an appealing option for producing sophisticated materials to prevent corrosion [7].

The current study aims to explore the synthesis of CdS by using sonochemical as a unique method, with particular focus on its potential use in corrosion prevention. Moreover, we extend the scope of our investigation by utilizing three different acidic, basic and neutral electrolytes during the synthesis process, aiming to reveal the distinctive characteristics and performance variations of the resultant CdS coatings. Thus, the comprehensive investigation of the synthesis of cadmium sulfide via the sonochemical method and its application for anticorrosion purposes using three distinct electrolytes have been examined and investigated using several physicochemical techniques such as X-ray diffraction technique with corresponding Rietveld refinement profile, FT-IR, Particle size analyzer (PSA), and optical properties examined through ultraviolet (UV)-visible spectroscopy and morphological study via SEM along with EDAX, scanning probe microscopy (SPM) and corrosion studies examined using different electrolytes.

EXPERIMENTAL

The cadmium chloride ($CdCl_2$), sodium sulphide flakes (Na_2S) and citric acid were purchased from Merck. To prepare CdS nanoparticles, double distilled water (DD) was used as a solvent. The CdS nanoparticles have been produced using the sonochemical route, and 0.01 M of $CdCl_2$ solution, 0.1 M of citric acid and 0.01 M of Na_2S solutions were prepared separately [8]. The $CdCl_2$ suspension was subjected to dropwise addition of citric acid, followed by stirring for a duration of 30 minutes, resulting in the formation of a homogeneous solution. After that, sodium sulphite solution was added to the above solution, which resulted in a yellow colour, and to improve the reaction with it, the final solution was agitated for 4 hours. The chemical reaction is as follows (Equation 1) [9].

$$CdCl_2 + Na_2S \rightarrow CdS + 2\ NaCl \quad (1)$$

A sonicator with a 40 KHz frequency was used to sonicate the prepared solution for one hour until an apparent yellow colour suspension resulted. After this suspension of precipitates was obtained, the base solution was dehydrated for 12 hours using an oven at 80 °C. For ultrafine CdS nanoparticles, the final sediment was dried in an oven at 120 °C for 6 hours. The graphic illustration of the CdS nanoparticles synthesis process is revealed in Figure 1.

Sample preparation for corrosion studies

The experimental investigation included the use of a mild steel (MS) metal plate to examine the anticorrosive properties of prepared CdS nanoparticles. The MS metal plate underwent a sequential polishing process using SiC grit papers of 9 mm, 3 mm, and 1 mm. After each polishing phase, the plate was washed using acetone, subsequently rinsed with DD water, and finally dried using an oven.

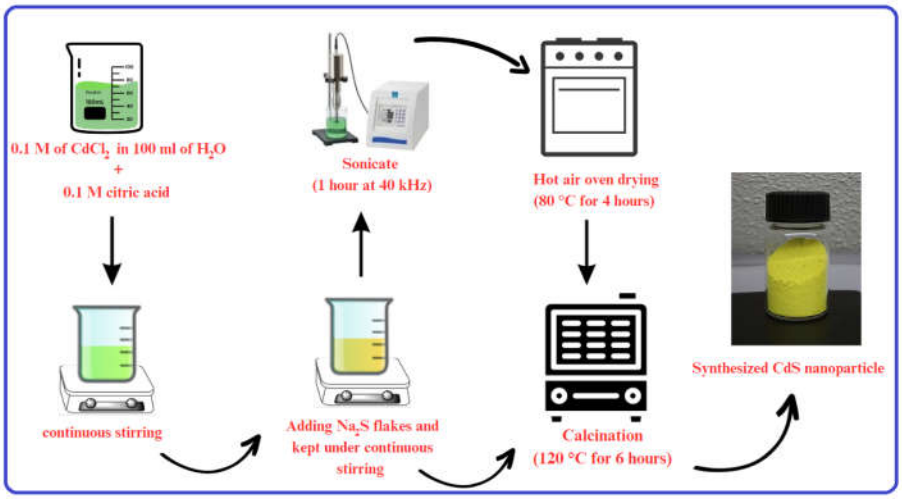

Figure 1. Synthesis of CdS nanoparticles.

Subsequently, a slurry was prepared by combining 15 mg of CdS nanoparticles with N-methyl-2-pyrrolidone and polyvinylidene difluoride in weight proportions of 80:15:5, respectively. The slurry was coated onto the surface of the MS metal plate, covering an area of 1 cm^2, with the doctor's blade procedure. The application of the coating was iterated 3 times in order to get a consistent thickness of about 1 mm of CdS NPs on the metal surface. The plate with a coating was imperiled to a drying process in an oven at 80°C for a duration of 1 hour. Subsequently, the plate was used for the purpose of investigating corrosion in the presence of four different electrolyte atmospheres.

Characterisation of CdS nanoparticles

The XRD was used to evaluate the phase clarity and assess the prepared CdS NPs' structural components with Cu anode. Rietveld refinement analytical method using FULLPROF software was performed to analyze the lattice parameter and crystal values of the prepared CdS nanoparticles. The FTIR (PerkinElmer, USA) study was conducted for functional group identification of the prepared CdS NPs. To know the average particle size distribution, a particle size analyzer (Nanophox; Sympatec, Germany) study was performed, at a wavelength of 633 nm using a laser beam by light scattering technique. The technique was performed several times to get the optimized data to acquire an average particle size. To study the optical absorbance of CdS nanoparticles, UV-Vis spectroscopy was performed and DD water as a solvent in the electromagnetic spectral wavelength ranging from 180 to 800 nm. The bandgap of CdS NPs is calculated with the results of UV-Vis spectroscopy by employing Tauc relations. Surface topology and morphological characteristics of CdS nanoparticles were considered using FESEM in addition

to EDX with elemental mapping analysis. Photoluminescence spectroscopy was used to investigate the electronic and optical properties of the synthesised CdS nanoparticles. The instrument used for this analysis was the Cary Eclipse, manufactured by Agilent Technologies in Singapore.

Electrochemical measurements

The electrochemical impedance spectroscopy (EIS) procedure was utilized to assess the anticorrosive properties of the coating [9]. The study focused on the corrosion characteristics of magnesium metal via a three-electrode cell configuration. A salt bridge was employed as a reference electrode within the overall setting of a sulfate electrolyte. An investigation of electrochemical corrosion was conducted, with experimentation continuing until reaching the level of the concurrent value through the Autolab equipment, namely the PGSTAT302N, Autolab, Netherlands using different electrolytes, acidic (HCl), basic (KOH), and neutral (NaCl). The range of applied potential used to investigate corrosion behaviours ranged from -1.8 to -1 V, with a 5 mV scanning rate. The corrosion current (I_{corr}) and corrosion potential (E_{corr}) were measured by extrapolating the data obtained from the anodic and cathodic regions of the potentiodynamic polarization test, also known as the Tafel plot [8]. A 5 mV amplitude alternating current was used to record the impedance data throughout a frequency spectrum of 0.01 to 100 kHz. The examinations were conducted three times to confirm the reliability of the findings.

RESULTS AND DISCUSSION

The occurrence of several diffraction peaks exhibiting a wide peak silhouette in the XRD band may be ascribed to the polycrystalline characteristics of the synthesised CdS nanoparticles. The Figure 2(a) displays the XRD pattern of the synthesised CdS nanoparticles.

The presence of a diffuse background in the X-ray diffraction spectrum might be attributed to the amorphous nature resulting from the lack of ordered periodicity in the lattice structure. This particular pattern of behaviour is often found in particles of nanoscale dimensions. This preferred orientation along the (0 0 2) plane of the wurtzite (α-CdS) crystal structure is confirmed by comparing the 2θ position of diffraction peaks and the XRD peak profile with standard JCPDS data. Furthermore, an additional peak has been seen at a 2θ value of 31.33°, which is indicative of hexagonal close-packed (HCP) CdS nanoparticles [10]. This observation suggests that the synthesised CdS nanoparticles possess a high concentration of cadmium (Cd) content. The observed intensity of diffraction peaks exhibits a significant decrease when compared to the bulk CdS material. Furthermore, the diffraction peaks seen in CdS nanoparticles display a notable displacement towards larger diffraction angles when compared to bulk CdS.

The observed phenomena might be explained by the lattice contraction that occurs as the surface-to-volume ratio of nanoparticles increases [11]. Using Bragg's diffraction equation, the values of the interplanar spacing 'hkl' have been determined. The synthesised CdS nanoparticles provide further evidence of lattice contraction due to the existence of lower hkl values compared to the standard hkl value. It was noted that the synthetic CdS NPs had lattice constants lower than the standard values. Given the reduced size of nanoparticles, it is reasonable to suppose that the lattice contracts due to defects such surface or interface tension, strain, and dislocations [12]. Figure 2(b) shows the X-ray diffraction pattern of cadmium sulphide after it has been refined using the Rietveld algorithm in the MAUD software. The narrow shape of the peaks detected in the CdS sample indicates that the size of the crystallites has increased noticeably.

The structural parameters of CdS nanoparticles such as crystal structure, space group, crystal size, lattice parameter a = b and c, volume, lattice strain, micro strain, dislocation density, R_p, R_{wp}, R_{exp} and Chi^2 are hexagonal, P63mc (186), 9.8, 4.135 and 6.71, 99.49, 0.0036, 0.22%, 1.17 $\times 10^{-3}$ $(nm)^{-2}$, 10.6, 13.5, 9.94 and 1.8, respectively. The CdS sample obtained through the ultrasonication-assisted approach was analysed using the X'pert High Score Plus programme.

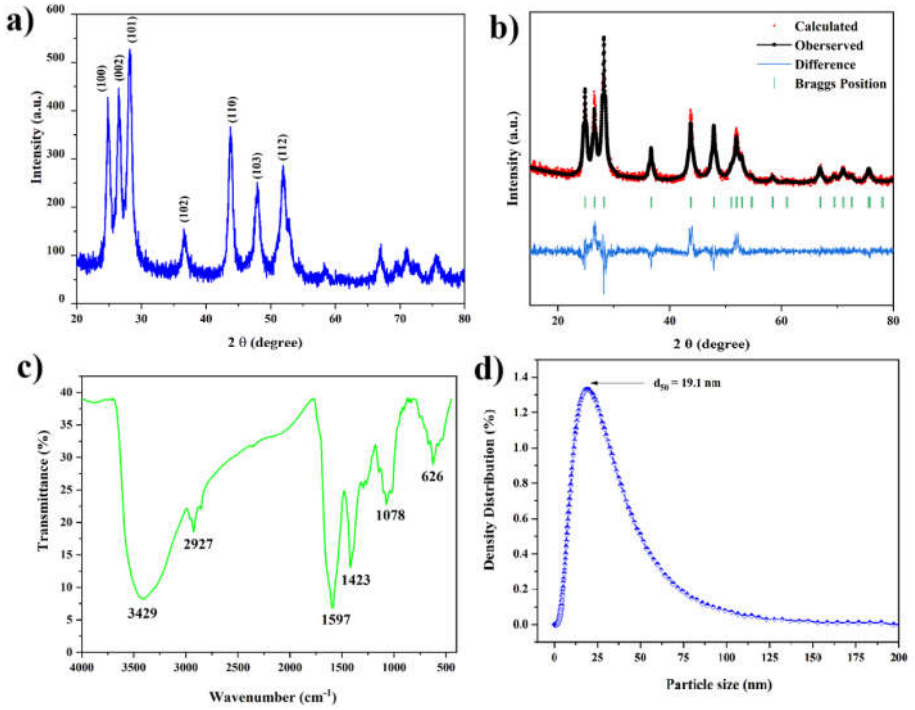

Figure 2. (a) XRD, (b) Rietveld refinement, (c) FTIR spectra, and (d) Particle size analysis of CdS nanoparticles.

The analysis revealed the presence of two distinct phases: hexagonal wurtzite with the space group P63mc. Through analysis of the FT-IR spectrum revealed that the synthesised CdS nanopowder exhibits several absorption peaks and bands. These spectral features may be attributed to the molecular alignment of the constituent components. Figure 2(c) displays the FTIR spectra of the synthesised CdS nanoparticles. The Cd–S stretching frequency typically appears to be positioned in the lower wavenumber range, namely below 700 cm^{-1} with a notable absorption peak at 651.62 cm^{-1}, which may be ascribed to the stretching of Cd–S bonds. The absorption peaks seen at 1075.85 and 1164.33 cm^{-1} may be attributed to the C–N stretch/C=S vibrations of thiourea. Additionally, the peak observed at 1374.15 cm^{-1} resembles to the tris-amine C–N stretch, which shares similarities with the C–O stretching vibrations. Additionally, there are peaks seen at 2000.37 and 2150.47 cm^{-1} which is associated with the N=C stretching or isothiocyanate (–NCS) group produced as a result of the hydrolysis of thiourea in the synthesis process [13]. The presence of a doublet of weak intensity at 2922.61 and 2854.01 cm^{-1} has been attributed to the asymmetrical and symmetrical vibrations of the CH group. Additionally, the asymmetric scissor deformation vibration is seen at 1444.50 cm^{-1}. The absorption bands seen at 3429.97 and 1628.95 cm^{-1} are attributed to the O–H stretching vibration of water molecules [14]. The presence of an additional absorption peak at 896.45 cm^{-1} may be attributed to the O–H out-of-plane bending vibration of water molecules, which exhibits relatively low intensity. The presence of moisture content in CdS nanoparticles has been reported to induce vibrations, which remain even after undergoing thermal annealing. The presence of distinct absorption peaks and bands seen in the FT-IR spectrum provides evidence for the existence of CdS molecules and traces of contaminants. These

observations may be attributed to the chemical reactions involving various precursors and the presence of water molecules or hydroxide ions during the synthesis of the nanoparticles [15].

The DLS approach is used to investigate the PSD of CdS nanoparticles that have been synthesised. The average PSD of all the synthesised CdS NPs is revealed in Figure 2(d). The nanoparticles were evenly distributed in deionized water with the use of gentle sonication for a duration of 10 minutes prior to conducting DLS examination. The Figure 2(d) illustrates variations in the diameters of CdS NPs tends to be more significant compared to the particle sizes derived from XRD data due to the effects of surface solvation and agglomeration of particles in colloidal solutions. The particle sizes exhibit a range varying from 11.1 nm to 75.9 nm and the mean PSD of the synthesised CdS nanoparticles is 19.1 nm which are perfectly matched with the XRD and earlier reports [16].

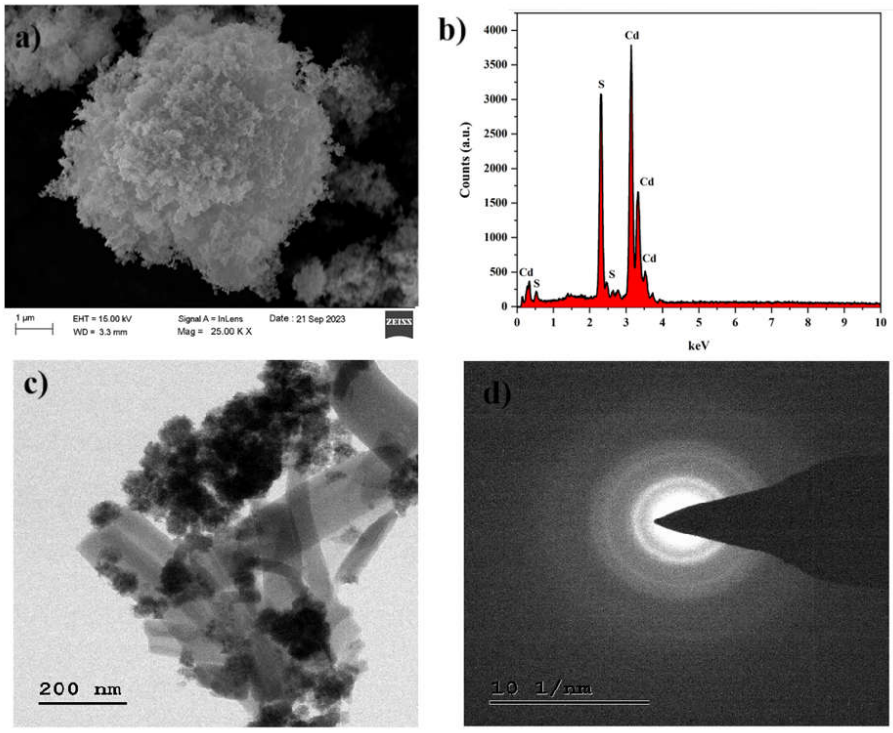

Figure 3. SEM and TEM images of prepared CdS nanoparticles.

The field emission image of CdS NPs is shown in Figure 3(a-b) depicts nanoparticles composed of Cd and S. The morphology of the nanoparticles that have been created is characterised by the presence of aggregates. The formation of these flocks is characterised by the dense aggregation of an unlimited number of crystallites. The formation of these dense clusters occurs in CdS powder as a result of uniform precipitation during the synthesis procedure, followed by the development of crystallites inside the clusters. The nano-crystallites are found inside the clusters and have a morphology resembling flakes. The identification of particles' shape, size, and boundaries in powder samples based on SEM pictures poses challenges. To address this issue, the ImageJ programme was used for image analysis [17]. The ImageJ application, with its analysis

function, determined the average size is 29.7 nm. The Figure 3(c-d) displays the TEM micrographs and SAED pattern of the CdS nanoparticles displaying the rod-like morphology with particle sizes less than 30 nm which revealed that the small sized CdS nanoparticles were formed when the ultrasonication process was involved in the synthesis procedure [16]. This means that the precipitation rate directly affected the particle size and it was found to be the lowest since precipitation appears to occur most rapidly in this instance. Additionally, the use of stabilisers resulted in a decrease in the agglomeration and coagulation of CdS nanoparticles.

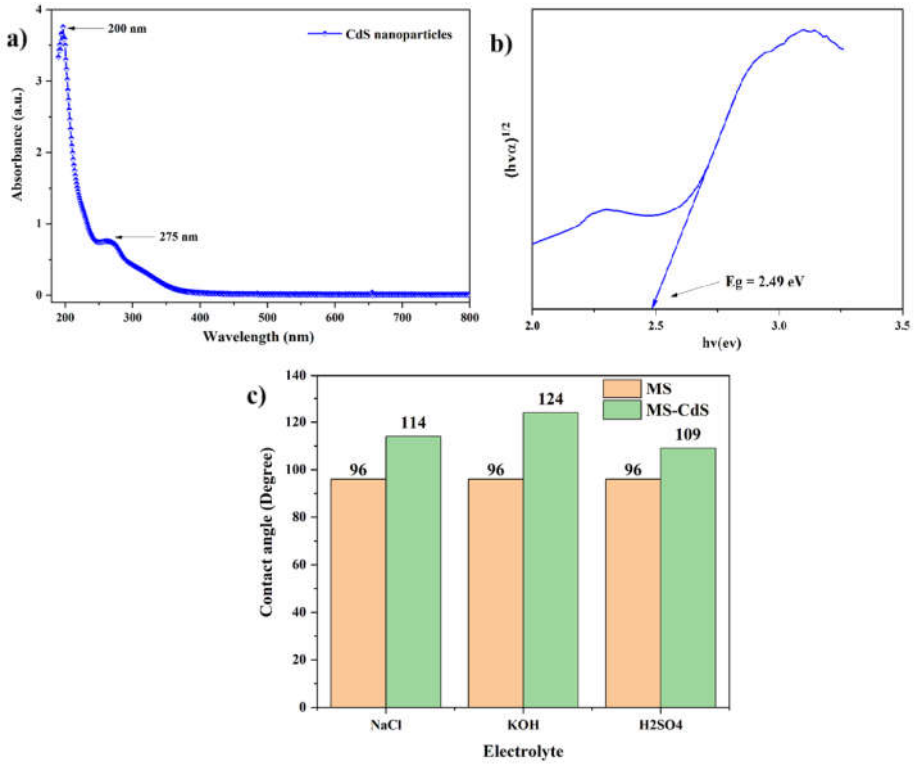

Figure 4. (a) UV Vis spectra, (b) Tauc plot for CdS nanoparticles, and (c) Contact angle analysis for uncoated and CdS nanoparticles coated MS plates under three electrolytes.

The optical characteristics of semiconductor nanoparticles are considered to be fundamental aspects. Figure 4(a) demonstrates the UV-Vis spectra of the CdS nanoparticles that were synthesised. In current compassion, there exists a well-recognised relation wherein the optical band gap of a semiconductor exhibits an increase when the particle size decreases, eventually converging towards the dimensions associated with the Bohr exciton. The phenomenon under consideration is characterised by an apparent shift of the absorption edge towards shorter wavelengths, often referred to as a blueshift in absorption spectra. The absorption spectrum shows a reduction in absorption as the wavelength of CdS nanoparticles increases. The study outcomes suggest that the CdS nanoparticles exhibit a high level of transparency in the visible area, as shown by an optical absorption rate of less than 20% [15]. In various semiconductor nanoforms, an excitation peak and ab-sorption edge are assessed by the second derivative of the absorption spectrum. The analysis reveals that the excitation peak can be observed with a wavelength of 190

nm, while the absorption edge is detected at wavelengths of 200 nm and 275 nm [12]. The observed phenomenon of a blue shift in the absorption edge seems to be a result of the quantum confinement effect, a phenomenon that is anticipated in nanoscale CdS particles. The optical band gap and particle size values of CdS in different nanoforms exhibit significant variations, dependent upon the specific synthesis procedure employed [11]. The present investigation included the determination of the optical bandgap of CdS NPs, revealing a value of 2.49 eV.

The characterization of the electronic transition occurring across the optical band gap may be determined by examining the wavelength-dependent behaviour of the optical coefficient. The determination of the transition's nature was conducted using the Tauc relation. Figure 4(b) illustrates the graphical representation of $(ah\gamma)^{1/2}$ plotted against $h\gamma$, where the point of intersection on the energy axis provides the direct bandgap energy (Eg) of the CdS nanoparticles. Notably, the observed shift in the band gap is towards larger values compared to previous findings and the bandgap energy of the nanoparticles was determined to be 2.49 eV.

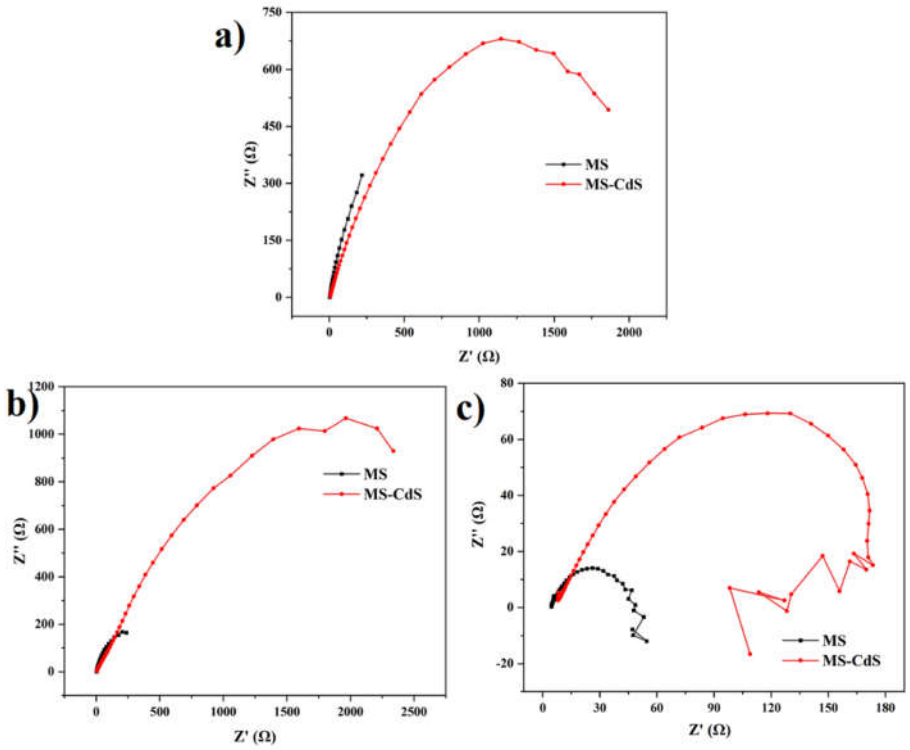

Figure 5. EIS plot (Nyquist plot) for uncoated and CdS nanoparticles coated MS plate in various aqueous electrolytes (a) 1 M H_2SO_4, (b) 1 M KOH, and (c) 3.5% NaCl.

The presented table demonstrates that the bandgap of CdS nanoparticles, which were synthesised, exhibited a greater value compared to the bandgap of bulk CdS (2.42 eV). Furthermore, it was observed that the bandgap energy got increasingly prominent as the particle size decreased. Therefore, it may be assumed that the synthesised CdS nanoparticles exhibited the phenomenon of quantum confinement [5]. The wettability of all the uncoated and CdS nanoparticles coated MS plate is determined through contact angle analysis, as shown in Figure

4(c). The CdS nanoparticles tend to be hydrophobic, and it improves super hydrophobic characteristics while coated on MS plate. The contact angle values are 96° for uncoated MS plates under all the electrolytes. Still, it moves to higher values such as 114°, 124°, and 109° for corresponding CdS nanoparticles coated plates under 3.5% NaCl, 3 M KOH and 1 M H_2SO_4 electrolytes, respectively. The CdS nanoparticles coating on MS plate could enhance their hydrophobic nature due to the presence of the polar surface group. Therefore, the improved wettability nature of the CdS-coated MS plate is highly suitable for anticorrosion applications because its hydrophobic nature may improve surface activities such as electrode-electrolyte interaction, ionic penetration and peel-off effects of coating. We can conclude that the CdS coating on the MS plate is highly stable under all electrolytes and didn't peel off during the analysis [7].

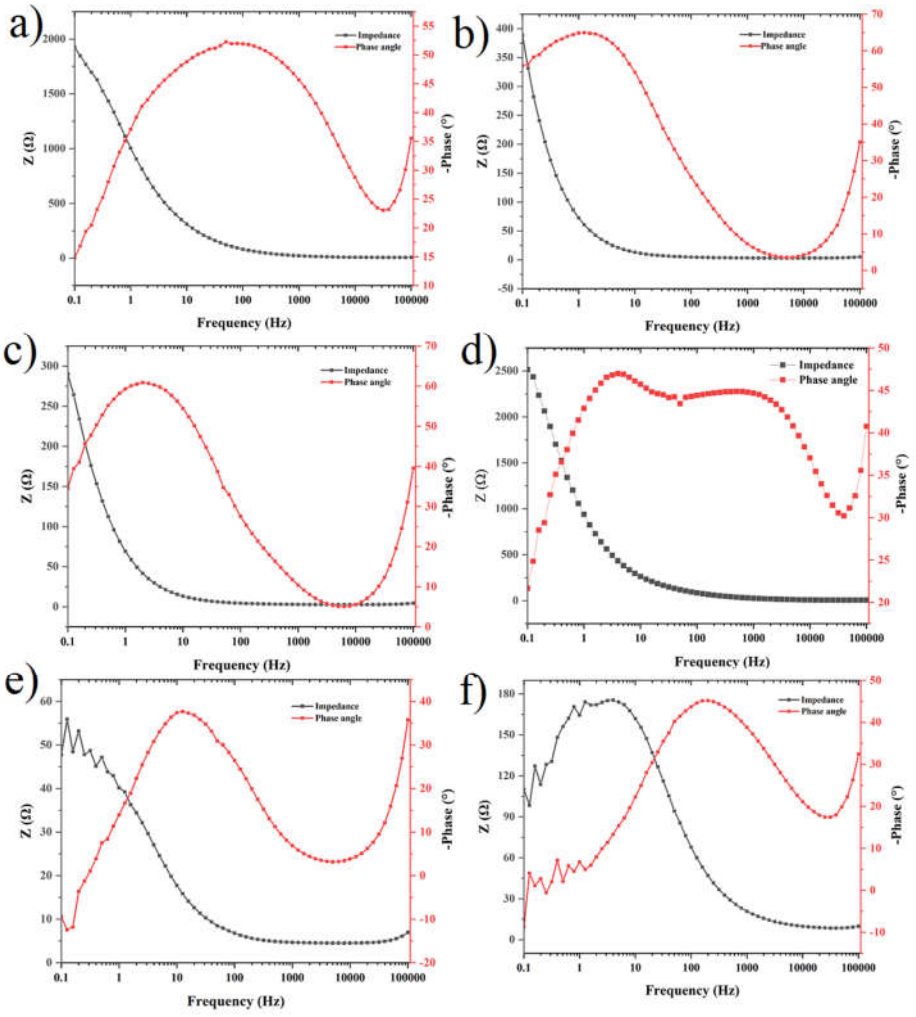

Figure 6. Bode plot for uncoated and CdS NPs coated MS plate in various aqueous electrolytes (a) 1 M H_2SO_4, (b) 1 M KOH, and (c) 3.5% NaCl.

Electrochemical and anticorrosion analysis

The electrochemical impedance spectra, also known as a Nyquist plot, are presented in Figure 5 (a-c) for uncoated and CdS nanoparticles coated MS plates under 1 M KOH, 1 M H_2SO_4 and 3.5% NaCl electrolytes. The plates immersed in the respective solutions measured these electrochemical impedance spectra.

In the Nyquist plot diagram, a half circle was created at low frequencies. This may have a linear relationship to the resistance of charge transfer in the reaction. Whether the plates are coated or uncoated has a discernible impact on the radii of the semicircles displayed by each sample in Figure 5. Loops of the electrical phenomenon were observed in every electrolyte that has been investigated. The Electrochemical Impedance Spectroscopy (EIS) is a reliable analytical testing method that may be utilized for corrosion investigation. This is because a non-destructive technique provides valuable information regarding electrochemical performance.

Figure 5(a-c) demonstrates the EIS analysis, and it displays the impedance of the uncoated electrode and the CdS nanoparticles coated electrode in the electrolyte throughout with a frequency range of 100 - 0.1 Hz. The electrolyte resistance (RS) values of all the samples exhibit a similar pattern, characterized by an elevated semicircle in the high-frequency range. The RS values of all the samples exhibited a uniform pattern, as seen by the depressed semicircle observed in the high-frequency region. The presence of the depressed semicircle plot is thought to be a result of the parallel combination of the charge transfer resistance (RCT) associated with the electrochemical process. The following equation suggests that the system's resistance is the primary factor in determining its impedance, denoted by Z [5].

$$Z = \frac{iR_{cT}}{1-\omega R_{cT}} \tag{2}$$

where, i represents the exchange current density of the redox process, the electrochemical behaviour and electrical features of the produced CdS-better electrode were demonstrated by the significantly reduced charge transfer resistance of EIS. The performance is superior to that of a MS substrate in terms of its ip and diffusion coefficient, as shown in Table 1, applied frequency (f) and capacitance (Cdl) when operating with an alternating sinusoidal potential. These findings are based on electrochemistry-related tests and estimates. The presence of a capacitive arc characteristic in the samples indicates corrosion prevention. However, specific samples as well display resistive features in high frequency region. This phenomenon has been seen in several samples, which has been related to the nonideality of the coatings in entirely hindering the corrosion types (such as oxygen, ions and water). Regarding the capacitive arc diameter, the resin-coated sample had roughly 11 times the diameter of the uncoated MS plate. This finding indicates that the CdS nanoparticles coating can protect the MS plate when it is in contact with the 1M H_2SO_4, 3 M KOH and 3.5% NaCl electrolyte. Compared to an MS plate not coated with CdS nanoparticles, the arc diameter was enhanced by 14 %.

Table 1. Electrochemical impedance parameters of uncoated and CdS nanoparticles coated MS plates under 1 M H_2SO_4, 3 M KOH, 3.5% NaCl electrolytes.

Electrolyte	Substrate	R_p		R_s	CPE.Y0	CPE.N
1 M H_2SO_4	MS	1293		3.2436	0.0012309	0.99605
	MS-CdS	2601.1		12.128	0.00016781	0.99342
3 M KOH	MS	439.63		3.6856	0.0036202	0.99618
	MS-CdS	3759.7		27.884	0.00024538	0.99333
3.5% NaCl	MS	52.789		4.2157	0.001357	0.99438
	MS-CdS	306.75		7.1211	0.00084369	0.99383

In order to enhance the study of the EIS data, Figures 6 a, b, and c exhibit the corresponding Bode magnitude and Bode phase plots. The Bode magnitude plot illustrates the relationship between the amplitude of alternating current and alternating voltage, as a function of frequency, without considering any phase shift. Conversely, the Bode phase diagram illustrates the differences in phase between the alternating voltage and AC current as a function of frequency, regardless of their respective amplitudes. Both graphs contain data that cannot be readily derived from Nyquist plots. The Figure 6 also exhibits an increase in impedance magnitude for CdS nanoparticles coated MS plates than uncoated MS plates. Despite this, the plots for all samples converge towards each other at the minimum frequency, with values ranging from 15 to 45 kΩ. The Bode phase graphs seen in Figure 6 serve as supplementary components of the EIS data. One notable attribute of the Bode phase plot is its capacity to recognize the typical electrical characteristics exhibited within a certain range of frequencies. For instance, the observed behaviours of capacitive, resistive, and mixed capacitive-resistive systems may be represented by lines with phase angles of -90 to 0, and 0 to -90º, respectively. The Bode phase graphs shown in Figure 6 exhibit distinct behaviour between samples of uncoated and CdS nanoparticles coated MS plate. The first knee observed for CdS nanoparticles coated MS plate, and more evident for uncoated MS plate, resembles to the capacitive-resistive transition of the Bode phase plots. Furthermore, the MS plate coated with CdS nanoparticles exhibits two-time constants that are of similar magnitude.

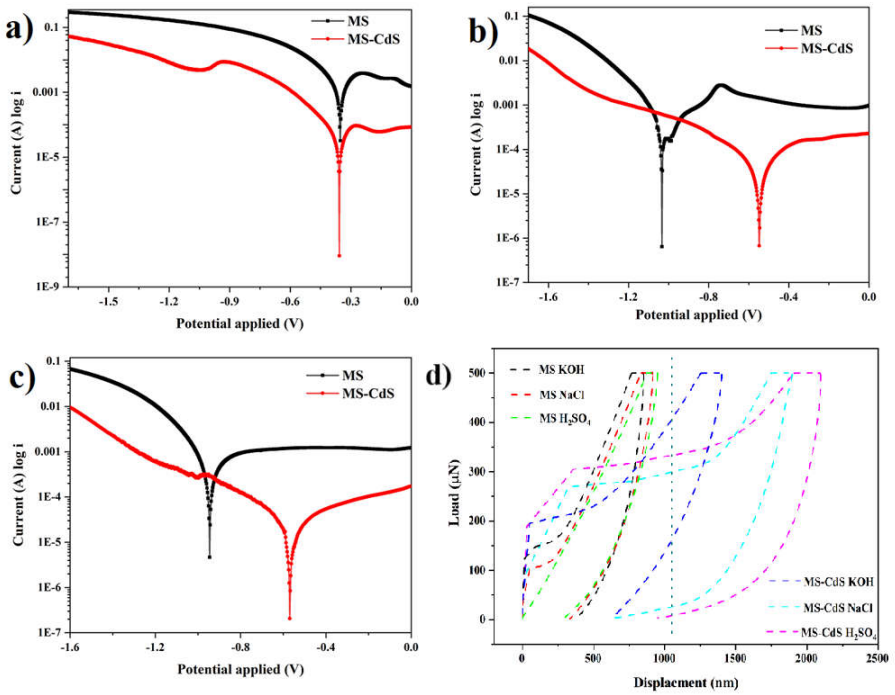

Figure 7. Potentiodynamic polarization for uncoated and CdS nanoparticles coated MS plate in various aqueous electrolytes (a) 1 M H_2SO_4, (b) 1 M KOH, (c) 3.5% NaCl and (d) Nanoindentation test images of uncoated and CdS nanoparticles coated MS plates under aqueous electrolytes (a) 1 M H_2SO_4, (b) 1 M KOH, (c) 3.5% NaCl.

The attribution of these two processes may be attributed to the contact between the coating and the electrolyte-CdS-CdS nanoparticles. The observed low resistance and high capacitance may be attributed to the significant porosity of the coating, which is reliable with the findings attained from the LSV analysis. The phase angle of -50º seen at high frequency for CdS nanoparticles deposited on an MS plate is indicative of the capacitor's characteristic. In the case of CdS nanoparticles coated on an MS plate, the presence of a phase angle of -75º at high frequencies indicates the behaviour of a pure capacitor which serves as an effective inhibiting coating. The slightly decreased efficiency shown by the CdS film when compared to the MS plate is an area of interest that demands more research and analysis. The data were analysed by fitting them to an electrical equivalent circuit in order to obtain more information from the EIS data. A circuit with a two-time constant configuration was used for this intent. Nevertheless, as a result of the presence of system heterogeneities, the alignment between the experimental and fitted values was inadequate. Consequently, the capacitor components were substituted by constant phase elements (CPE). Within the analogous circuit, Rs denotes the resistance of the solution or electrolyte, whereas Rp represents the resistance associated with polarization. Table 2 displays the values of CPE, Rs, and Rp. It is evident that there was a significant rise in the resistance (Rp) upon the application of CdS nanoparticles onto the metal substrate (MS plate). The relationship between Rp and coating resistance is apparent, indicating a better efficiency of the CdS nanoparticles coated MS plate in comparison to the uncoated MS plate. The Figure 7(a-c) depicts the potentiodynamic polarization curves, known as Tafel plots, of uncoated and CdS nanoparticles, coated MS plates in electrolytic solutions of 1 M H_2SO_4, 3 M KOH, and 3.5% NaCl, respectively. The electrochemical corrosion parameters, such as corrosion potential (E_{corr}), corrosion rate (CR), corrosion current (I_{corr}), and polarization resistance (R_{pol}), were determined using the Tafel plot, and the results are presented in Table 2. The electrochemical corrosion inhibition behaviours of MS plates are conferred in an electrolyte-wise fashion for the sake of ease of comprehension.

Table 2. Potentiodynamic polarization parameters under 1 M H_2SO_4, 3 M KOH, 3.5% NaCl electrolytes.

Electrolyte	Substrate	ba (dec)	bc (dec)	E_{corr} (V)	I_{corr} (A) (x E-05)	Polarization resistance (Ω)	Corrosion rate (mm/y)	Efficiency (%)
1 M H_2SO_4	MS	0.1342	0.1356	-0.353	1.4235	20.586	16.541	95.72
	MS-CdS	0.1853	0.1803	-0.357	5.8526	678.12	0.680	
3 M KOH	MS	0.1832	0.1255	-1.036	4.9259	65.706	5.723	96.17
	MS-CdS	0.0927	0.1072	-0.546	1.8901	1142.7	0.219	
3.5% NaCl	MS	0.2082	0.1248	-0.943	4.0348	84.03	4.688	96.94
	MS-CdS	0.1361	0.1129	-0.573	1.2329	2174.9	0.143	

When CdS nanoparticles coated MS plates were placed in 1 M H_2SO_4 alongside uncoated MS plates, the polarization resistance of the coated plates increased, which decreased the corrosion rate of the coated plates. These findings demonstrated that a coating of CdS nanoparticles applied on MS plates suggestively impacted the corrosion rate. Because of their larger surface area and porous character, the CdS nanoparticles that have been created can effectively adsorb and repel the hydrogen and sulfur ions present in the H_2SO_4 electrolyte. In contrast, the corrosion potential of MS and MS-CdS plates in 3 M KOH media was around 4.9259 V and 1.8901 V, respectively. This was the case when the plates were tested. Compared to the uncoated MS plate's values, the MS-CdS plate's corrosion potential values were much lower than those of the uncoated MS plate.

On the other hand, the potential for corrosion of MS-CdS plates moved into a region that was more negative than that of MS. In the electrolytic medium of KOH, the uncoated MS plate showed a significant corrosion rate of 5.723 mm/year and a substantial polarisation resistance of 65.706. On the other hand, the MS-CdS plate exhibited a corrosion rate of 0.219 mm/year, indicating a relatively low level of corrosion. Additionally, it had a high polarisation resistance value of 1142.7

Ω. These results were in comparison to the uncoated MS plate's results. The results presented above demonstrate that a thin layer coating of CdS nanoparticles can be applied to the surface of MS metal plates to achieve a low corrosion rate and a strong resistance to electrochemical corrosion.

The potentiodynamic polarization investigations of MS and MS-CdS metal plates found that the MS-CdS metal plates were more anodically polarized than the uncoated MS metal plates when used in an electrolytic solution containing 3.5% NaCl. These findings were based on the results of the studies. Compared to pure MS plates, the coated plates tend to limit the corrosion process. It has been determined that the corrosion potential, or E_{corr}, of the MS-CdS samples is superior to that of the uncoated MS plates. This suggests that the MS-CdS plates, which have a corrosion rate of 0.143 mm/year, are superior to the pure plates, which have a rate of 4.688 mm/year. The oxygen reduction of Cd^{2+} ions led to an increase in the MS-CdS plates' polarisation resistance compared to the MS samples which indicates that MS and MS-CdS plates have a superior ability to suppress corrosion.

The comprehensive analysis of the relative effectiveness of various nanomaterial coatings on various metal surfaces in terms of their ability to stop corrosion shows that nanoparticle coatings made of metal oxides, specifically SnO_2, Al_2O_3, NiO-Zn, and ZrO_2, reduce the corrosion rate by 59.8%, 51.7%, 49.7%, and 69.1%, respectively. In our experiment, a CdS nanoparticles-coated MS plate exhibited corrosion inhibition activity at 95.72%, 96.17%, and 96.94% when subjected to 1M H_2SO_4, 3M KOH, and 3.5% NaCl electrolytes. This demonstrates that the produced CdS nanoparticle may effectively stop the corrosion of mild steel under various conditions.

Figure 7(d) depicts the findings of nanoindentation performed on a CdS nanoparticles-coated MS plate both before and after electrochemical measurements. The load-displacement curve exhibited consistent repeatability of surface coatings while the experimental settings were the same, as seen by the indentation of each five-point result. After undergoing electrochemical testing, it was discovered that the coated plates' hardness and roughness values had experienced a marginal improvement. When the MS plates were subjected to the LSV tests, the CdS nanoparticles coating provided high protection to the plates' surfaces. Ions from the corrosive medium in electrolytes, such as potassium, sodium, and sulphur ions, were swiftly diffused by the CdS nanoparticles due to their wide surface area and a high degree of stability.

Table 3. Nanointendation parameters of uncoated and CdS nanoparticles coated MS plates under H_2SO_4, KOH and NaCl electrolytes.

Electrolyte	Substrate	Displacement (nm)	Hardness (Pa)	Contact depth (nm)	Contact stiffness (μN/nm)	Roughness Ra (nm)
1M H_2SO_4	MS	1889.2	7.68	1887.4	1.4	89.5
	MS-CdS	2092.1	5.71	1626.3	1.3	104.9
3M KOH	MS	766.6	40.37	709.7	2.2	73.4
	MS-CdS	911.8	38.57	726.2	1.7	86.1
3.5% NaCl	MS	944.64	38.65	725	1.5	79.7
	MS-CdS	1354.7	16.05	1125.4	1.2	92.6

Before and after corrosion tests are shown in Table 3, which compares the hardness values, contact depth, contact stiffness, and surface roughness of uncoated and CdS nanoparticle-coated MS plates. Plates with CdS nanoparticles coated on them have significantly higher values than plates with surface roughness results comparable to those of the SPM experiments. The CdS nanoparticles that were prepared exhibited notable improvements in the corrosion inhibition properties of MS metal plates. This was determined by analysing wettability, electrochemical corrosion, and surface roughness. The nanoparticles' high surface area and stability in the water medium were identified as key factors contributing to their effectiveness. Compared with an

uncoated plate, the coated plate exhibits a more dramatic increase in the surface displacement that occurs in response to an applied load. In a manner very similar, the electrolyte contributes significantly to the process of degrading the surface of the coating. For an H_2SO_4 electrolyte, the surface roughness of an uncoated MS plate is measured at 89.5 nm, while a CdS nanoparticles-coated MS plate measures 104.9 nm. Similarly, the surface roughness of uncoated plates is measured to be either 73.4 nm or 79.7 nm when subjected to electrolytes consisting of 3M KOH or 3.5% NaCl. However, following the coating procedure, the surface's roughness value gradually increases due to the fine coating of CdS NPs. During the electrochemical reaction process, CdS-coated MS plates would inevitably see an increase in surface roughness.

CONCLUSION

The ultrafine CdS nanoparticles with a rod-shaped mixed flake-like morphology were prepared using a chemical approach that involved sonication to assist in the preparation. The effect of ultrasonication waves resulted in the CdS nanoparticles exhibiting enhanced crystallinity, increased purity, more significant surface area, and lower crystal and particle sizes. The reduction in crystal size brought about these changes. The results of SEM microscopy and nanoindentation techniques agreed with the hypothesis that the CdS nanoparticle deposition on the surfaces of MS metal plates was stable. In contrast to the qualities displayed by the CdS nanoparticles when exposed to the other electrolyte mediums, the CdS nanoparticles produced and deposited as a coating on MS metal plates showed outstanding corrosion prevention properties when subjected to a NaCl medium. According to the findings, the corrosion resistance was significantly improved by 96.94% after being subjected to a NaCl solution containing 3.5 wt.%. When exposed to 1 M H_2SO_4 and 3 M KOH solutions, the material's corrosion resistance improves by 95.72% and 96.17%, respectively. The high stability of the CdS nanoparticles coating can be seen in the surface profiles of the coated plates. These surface characteristics include roughness, hardness, and stiffness. Based on the aforementioned experimental evaluation, it has been determined that the preparation of CdS nanoparticles through a sonication-assisted simple chemical method shows promise as a viable option for enhancing the corrosion prevention properties of MS metals in various electrolytic environments. When magnesium metal plates were subjected to solutions containing sodium chloride, hydrochloric acid, and potassium hydroxide, the results showed that these compounds functioned very effectively as corrosion inhibitors for the magnesium metal plates.

ACKNOWLEDGEMENTS

The authors (Sultan Althahban, Mohammed Kuku, Yosef Jazaa) extend their appreciation to the deputyship for research and innovation, ministry of education in Saudi Arabia for funding this research work through the project number ISP-2024. This research also supported by Basic Science Research Program through the National Research Foundation of Korea (NRF) funded by the Ministry of Education (NRF-RS-2023-00237287, NRF-2021S1A5A8062526) and local government-university cooperation-based regional innovation projects (2021RIS-003) through the corresponding author (Haewon Byeon).

REFERENCES

1. Kong, Z.; Jin, Y.; Sabbir Hossen, G.; Hong, S.; Wang, Y.; Vu, Q.V.; Truong, V.H.; Tao, Q.; Kim, S.E. Experimental and theoretical study on mechanical properties of mild steel after corrosion. *Ocean Eng.* **2022**, 246, 110652.

2. Nawaz, M.; Akhtar, S.; Qureshi, F.; Almofty, S.A.; Nissapatron, V. Preparation of indium-cadmium sulfide nanoparticles with diverse morphologies: Photocatalytic and cytotoxicity study. *J. Mol. Struct.* **2022**, 1253, 132288.
3. Dong, G.; Wang, H.; Yan, Z.; Zhang, J.; Ji, X.; Lin, M.; Dahlgren, R.A.; Shang, X.; Zhang, M.; Chen, Z. Cadmium sulfide nanoparticles-assisted intimate coupling of microbial and photoelectrochemical processes: Mechanisms and environmental applications. *Sci. Total Environ.* **2020**, 740, 140080.
4. Sun, C.; Karuppasamy, L.; Gurusamy, L.; Yang, H.J.; Liu, C.H.; Dong, J.; Wu, J.J. Facile sonochemical synthesis of CdS/COF heterostructured nanocomposites and their enhanced photocatalytic degradation of bisphenol-A. *Sep. Purif. Technol.* **2021**, 271, 118873.
5. Zhang, K.; Lu, G.; Xi, Z.; Li, Y.; Luan, Q.; Huang, X. Covalent organic framework stabilized CdS nanoparticles as efficient visible-light-driven photocatalysts for selective oxidation of aromatic alcohols. *Chin. Chem. Lett.* **2021**, 32, 2207–2211.
6. Abd, M.S.; Wasly, H.S.; Batoo, K.M. X-Ray peak profile analysis and optical properties of CdS nanoparticles synthesized via the hydrothermal method. *Appl. Phys. A: Mater. Sci. Process.* **2019**, 125, 283.
7. Meng, L.; Lane, J.M.D.; Baca, L.; Tafoya, J.; Ao, T.; Stoltzfus, B.; Knudson, M.; Morgan, D.; Austin, K.; Park, C. Shape dependence of pressure-induced phase transition in CdS semiconductor nanocrystals. *J. Am. Chem. Soc.* **2020**, 142, 6505–6510.
8. Altun, B.; Ajjaq, A.; Çağırtekin, A.O.; Er, I.K.; Sarf, F.; Acar, S. Influence of isovalent Cd doping concentration and temperature on electric and dielectric properties of ZnO films. *Ceram. Int.* **2021**, 47, 27251–27266.
9. Chen, J.; Wu, Y.; Lei, Y.; Du, P.; Li, C.; Du, B.; Wang, Y.; Luo, L.; Bao, S.; Zou, B. The effects of Zn/Cd ratio and GQDs doping on the photoelectric performance of ZnxCd1-xSe. *Mater. Sci. Eng. B* **2022**, 286, 116058.
10. Diliegros-Godines, C.J.; García-Zaldivar, O.; Flores-Ruiz, F.J.; Fernández-Domínguez, E.; Torres-Delgado, G.; Castanedo-Pérez, R. Impedance Spectroscopy of Au/Cu_2Te/CdTe/CdS/Cd_2SnO_4/glass solar cells. *Ceram. Int.* **2023**, 49, 6699–6707.
11. Xie, R.; Tang, B. Influence of surface roughness on concrete nanoindentation. *Eur. J. Environ. Civ. Eng.* **2022**, 26, 3818–3831.
12. Charvatova Campbell, A.; Bursikova, V.; Martinek, J.; Klapetek, P. Modeling the influence of roughness on nanoindentation data using finite element analysis. *Int. J. Mech. Sci.* **2019**, 161-162, 105015.
13. Kolodin, A.N.; Bulavchenko, A.I. Contact angle and free surface energy of CdS films on polystyrene substrate. *Appl. Surf. Sci.* **2019**, 463, 820–828.
14. Wu, H.; Li, Y.; Feng, W.; Zhong, X.; Li, J.; Liu, S.; Liu, H.; Ma, G.; Xie, R. Three-dimensional zinc oxide decorated with cadmium sulfide nanoparticles heterogenous nanoarchitectures with expedited charge separation toward efficient photocatalytic degradation of organic pollutants. *Mater. Sci. Eng. B* **2023**, 292, 116459.
15. Acero-Gutiérrez, A.K.; Pérez-Flores, A.L.; Godínez-Salcedo, J.G.; Moreno-Palmerin, J.; Morales-Ramírez, Á. de J. Corrosion protection of A36 steel with SnO_2 nanoparticles integrated into SiO_2 coatings. *Coat. World* **2020**, 10, 385.
16. Cui, L.Y.; Wei, G.B.; Zeng, R.C.; Li, S.Q.; Zou, Y.H.; Han, E.H. Corrosion resistance of a novel SnO_2-doped dicalcium phosphate coating on AZ31 magnesium alloy. *Bioact. Mater.* **2018**, *3*, 245–249.
17. Chiu, L.H.; Chen, C.C.; Yang, C.F. Improvement of corrosion properties in an aluminum-sprayed AZ31 magnesium alloy by a post-hot pressing and anodizing treatment. *Surf. Coat. Technol.* **2005**, *191*, 181–187.